Automatic Detection of Targets Using Center-Surround Difference and Local Thresholding

Sun-Gu Sun
Agency for Defense Development, Yuseong P.O. Box 35-1, Daejeon, Korea
Email: sgsun@add.re.kr

Dong-Min Kwak
Agency for Defense Development, Yuseong P.O. Box 35-1, Daejeon, Korea
Email: imis@add.re.kr

***Abstract*—This paper proposes a new target detection method in low contrast forward looking infrared (FLIR) images. Automatic detection of small targets in remotely sensed images is a difficult and challenging work. The goal is to find out target locations with low false alarms in a thermal infrared scene of battlefield. The interesting targets are military vehicles such as battle tanks and armored personal carriers in ground-to-ground scenarios. The proposed method consists of three following stages. First, center-surround difference is proposed in order to find salient areas in an input image. Second, local thresholding for a region of interest (ROI) is proposed. The ROI is selected on the basis of a salient region that is the result of first step. Third, the shape of extracted binary images is compared with binary target templates using size and affinity to remove clutters. In the experiments, the proposed method is compared with morphology method using many natural infrared images with high variability. The result demonstrates that our method is superior to the morphological method in terms of receiver operating characteristic (ROC) curve and average computation time.**

***Index Terms*— binary template matching, center-surround difference, forward looking infrared, local thresholding, target detection**

I. INTRODUCTION

A human being can recognize different objects in relatively visible and peaceful environments. However, human capability is drastically deteriorated in low visible environment or in hazardous circumstance such as battlefield. To compensate for such limitations of human, intelligent and versatile automatic target recognition (ATR) is required [1-4]. ATR is a task that finds out target locations and identifies the types of targets. In the near future, ATR system will be an extremely important component for a variety of defense systems such as battle tanks, aircrafts and ships.

For instance, an ATR system of battle tanks may reduce the workloads of commanders significantly by suggesting effective responses in real time. ATR system uses various sensors like visible electro-optical (EO) sensor, laser radar and infrared sensor. Among these sensors, infrared sensors mounted on defense systems have an important role to watch and identify objects in unlit areas. However, automatic target detection and recognition are very difficult tasks in remotely sensed forward looking infrared (FLIR) images because the images contain numerous artifacts such as background clutters, target signature variability, various aspect angles and partial occlusion [5-20]. Figure 1 shows an example of FLIR image sensed by an infrared thermal sensor mounted on a military vehicle.

Typical ATR system consists of several stages: target detection stage that extracts regions containing potential targets in an image, clutter rejection stage that attempts to classify true targets by discarding the clutters from the potential targets provided by the detection stage, and classification stage that computes a set of features and determines the types of targets. This research focuses on the initial target detection and clutter rejection in Fig. 2.

Many researchers have developed various target detection algorithms in FLIR images. For example, typical methods are hit-miss transform, morphological wavelet [5], morphology [21], and directional wavelet [22]. To reject clutters in potential targets, S. A. Rizvi *et al*. proposed neural network approach using principal component analysis [18, 23], and L. A. Chan *et al*. used eigenspace separation transform [24] in the last few years. These methods dealt with considerably large targets with about 70 × 40 (width × height) pixels in FLIR images. However, our interesting target size is less than or equal to 30 × 15 pixels in the image. Generally, a crew of military systems would like to observe targets as far as possible. The images sensed in long distance have small targets and numerous clutters. And the images are low contrast and blurred. Therefore, detecting small targets in natural field images is more difficult and important than detecting large targets in military application.

Based on "Small target detection using center-surround difference with locally adaptive threshold", by Sun-Gu Sun, Dong-Min Kwak, Won Bum Jang, and Do-Jong Kim which appeared in the Proceedings of the IEEE International Symposium on ISPA 2005, Zagreb, Croatia, September 2005. © 2005 IEEE.

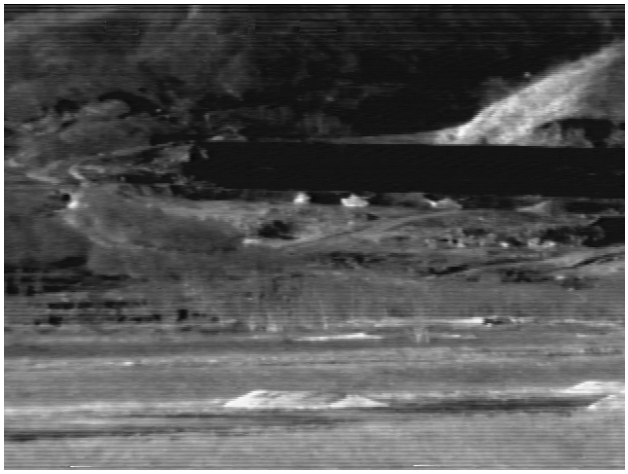

Figure 1. An example of FLIR image

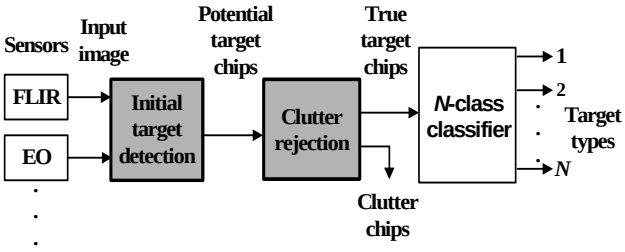

Figure 2. Block diagram of a typical ATR system

We are interested in thermal infrared images which are sensed by a panoramic sight mounted on a military vehicle. The input image is provided in the form of eight bit gray scale and digitized at 640 × 480 resolution. The target size varies from 10 × 8 to 30 × 15 pixels in an image. It is dependent on the range of interesting targets.

We propose center-surround difference and local thresholding as an initial target detector, and binary template matching as a clutter rejecter. Center-surround difference in the Gaussian pyramid of an input image is presented in Sec. II.A. Section II.B describes the proposed local thresholding using membership function with similarity and adjacency. Section II.C defines binary templates and an affinity measure to reject clutters from potential targets. Performance of the proposed method is compared with that of morphological method [21] in Sec. III. The test images are low contrast and high cluttered images gathered in various conditions such as different seasons, different times of the day, different ranges, and various aspect angles. Finally, conclusion is described in Sec. IV.

II. THE PROPOSED TARGET DETECTION METHOD

The proposed method consists of sequential three stages, that is, center-surround difference operation, local thresholding and binary template matching. Flowchart of the proposed method is shown in Fig. 3.

The previous methods of object detection tried to find salient areas in an image. However, Itti's method [25] was limited to find the most salient position in an image during one processing.

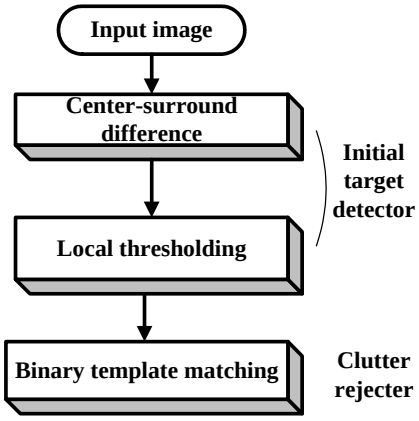

Figure 3. Flowchart of the proposed method

In fact, because intensity of targets in natural FLIR images is sometimes lower than that of background, the most salient position is liable to be selected out of clutters in the previous approaches. Moreover, to find many salient areas, user should predetermine the number of iteration of processing related to the number of interesting targets. That is, the number of potential targets to be detected has to be predetermined in the previous methods [25, 26]. To overcome this weakness of previous approaches, we propose center-surround difference operation with adaptive threshold. The method can be easily adapted to detect salient regions in low contrast and high cluttered images.

A. Center-surround difference

From an infrared image, Gaussian pyramid with seven spatial scales for intensity is made. Figure 4 shows an example of the Gaussian pyramid which is obtained by progressive low-pass filtering and sub-sampling of the input image [27]. Images, I_1 to I_6, are made by horizontal and vertical image reduction which factors are from 1:1 (scale zero) to 1:64 (scale six). An intensity feature map is made by center-surround difference operation. Center-surround difference is implemented by the pixel difference between fine and coarse scales. The following is detailed procedure for the center-surround difference.

Step 1: Compute center-surround difference by (1). The center is a pixel at scale $c \in \{1, 2, 3\}$ and the surround is the corresponding pixel at scale $s = c + \delta$ with $\delta \in \{2, 3\}$.

$$I_{c,s}(x,y) = \left| I_c(x,y) - I_s(x,y) \right|. \qquad (1)$$

I_s has to be interpolated so that the size is scale c to compute pixel difference. As the result of (1), six difference-maps, D_i, $i = a,\ldots,f$, are made by (2).

$$\begin{aligned} D_a &= I_{1,3},\ D_b = I_{1,4}, \\ D_c &= I_{2,4},\ D_d = I_{2,5}, \\ D_e &= I_{3,5},\ D_f = I_{3,6}. \end{aligned} \qquad (2)$$

Step 2: Normalize each D_i map by maximum dynamic range so that the feature value is ranged from 0 to 1. The normalized feature map N_i is computed by (3).

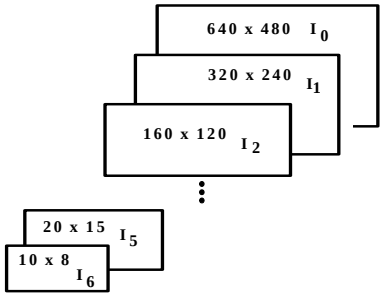

Figure 4. Gaussian pyramid of an image

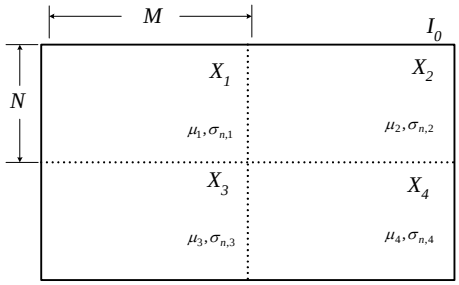

Figure 5. Four divisions of an input image

$$N_i(x,y) = \{D_i(x,y) - d_{\min}\}/(d_{\max} - d_{\min}), \quad (3)$$

where $d_{\max}$ and $d_{\min}$ are maximum and minimum difference.

Step 3: Interpolate each N_i map repeatedly to obtain feature maps with scale zero. The feature map is called F_i.

Step 4: Divide an original input image into four regions as shown in Fig. 5 so that salient areas are found with relation to the local variance of an input image. The normalized standard deviation for each region, $\sigma_{n,j}$, j =1,…,4, is computed by (4) to (6).

$$\mu_j = \frac{1}{M \times N} \sum_{y=0}^{N-1} \sum_{x=0}^{M-1} X_j(x,y), \quad (4)$$

$$\sigma_j^2 = \frac{1}{M \times N} \sum_{y=0}^{N-1} \sum_{x=0}^{M-1} [X_j(x,y) - \mu_j]^2, \quad (5)$$

$$\sigma_{n,j} = \sigma_j / 255, \quad (6)$$

where 255 is the maximum gray level of an image in (6). Local standard deviations are used for finding salient areas in an image because image characteristic of each region is very different from that of other regions due to wide field of view of imaging sensor.

Step 5: Obtain binary image B_i for each F_i by thresholding by (7). The threshold value is iteratively determined by weighting the normalized standard deviation through (8) to (10). Weighting coefficient ω_1 is iteratively changed so that near constant number of salient regions can be found.

$$\begin{aligned} B_i(x,y) &= 1 \ \text{ if } F_{i,j}(x,y) \ge t_j \\ &= 0 \ \text{ otherwise,} \end{aligned} \quad (7)$$

$$t_j = \omega_1 \times \sigma_{n,j}. \quad (8)$$

Step 6: Make a combined binary salient map $B(x,y)$ by binary OR operation of each pixel for six B_i maps as (9).

$$B(x,y) = \text{Binary OR}\{B_i(x,y)\} \ \ i = a,..., f \quad (9)$$

Step 7: Label [28] binary objects of the $B(x,y)$. The locations with "binary 1" in $B(x,y)$ are salient regions of an input image. The large binary objects can be included in the binary salient map B. Because locations of the large objects may be background in an input image with high probability, the large binary objects should be removed. To do this, a prior knowledge about maximum target size is used. During labeling of binary salient map B, we remove the objects that are larger than twice of the maximum target size in our implementation. It is necessary to shorten the processing time of next steps.

Step 8: Repeat from step 5 to step 7 and change ω_1 during each iteration by (10) unless the number of salient regions is greater than T_0 or ω_1 is less than ω_{th}.

$$\omega_1 = \omega_1 - \varepsilon. \quad (10)$$

We set ε=0.2, T_0=40, ω_{th}=3.0 and initial value of ω_1=3.6 in our implementation. This algorithm requires specification of these four parameters. Determination of initial value of ω_1 and ε is fully related to the number of iteration. However, T_0 and ω_{th} are related to the number of salient regions. Selection of T_0 and ω_{th} changes false alarms and execution time of following processing. T_0 and ω_{th} are determined by experiments. Figure 6 shows the result of center-surround difference of Fig. 1. The locations of white areas approximately represent salient regions of an input image.

B. Local thresholding

The previous thresholding methods based on histogram of an image are not suitable for our application because a region of interest (ROI) has small number of pixels. Therefore, we propose a new thresholding method utilizing pixel intensity and adjacency. Because intensity of an object in infrared images varies severely the adjacency is useful to extract a target from images. The detailed procedure of local thresholding is presented as follows:

Step 1: Select an ROI based on a salient region that is the reference region, R_r, as shown in Fig. 7. The reference region is white regions on the binary image in Fig. 6. $X_{\max}$ and $Y_{\max}$ stand for maximum width and height of targets in Fig. 7.

Step 2: Compute similarity of each pixel by (11) in the ROI.

$$S(g, g_r) = 1 - |g_{\max} - g| / c_1, \quad (11)$$

$$c_1 = g_{\max} - g_{\min}. \quad (12)$$

g is intensity of a pixel and $g_{\min}$ is minimum intensity in the ROI. And $g_{\max}$ is the maximum intensity in the reference region. Then, similarity is from 0 to 1. 1 means that the intensity of current pixel is same with the maximum intensity of reference region.

Step 3: Compute adjacency of a pixel based on the seed position by (14). If the distance from a pixel position (x,y) to the seed position (x',y') is d, it is given by (13).

$$d[(x,y),(x',y')] = \sqrt{(x-x')^2 + (y-y')^2}. \quad (13)$$

Figure 6. Result of center-surround difference of Fig. 1

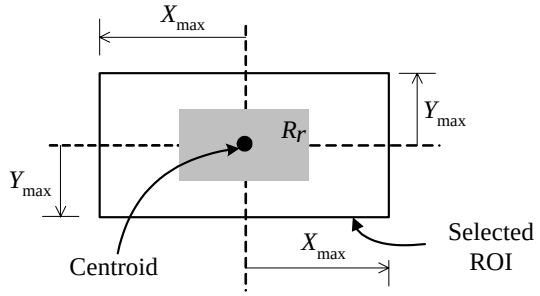

Figure 7. Selection of ROI

$$A[(x,y),(x',y')] = 1 \text{ if } d = 0$$
$$= \frac{2}{1+\sqrt{d[(x,y),(x',y')]}} \text{ otherwise,} \quad (14)$$

where (x',y') is the seed position that is centroid of the reference region. Adjacency ranges from 0 to 1.

Step 4: Compute membership value, μ, of a current pixel $g(x,y)$ by (15).

$$\mu[g(x,y)] = \beta \times S(g, g_r) + (1-\beta) \times A[(x,y),(x',y')], \quad (15)$$

where β is set to 0.6 and determined by experiments. Membership value is $0 \le \mu\ [g(x,y)] \le 1$.

Step 5: Make a binary image for the membership value by (16). If the membership value of a pixel is greater than 0.5, the pixel is classified as "binary 1" that means potential target pixel. Otherwise, the pixel is classified as "binary 0" that means background pixel. The threshold value is 0.5 so that thresholding is happened at maximum fuzziness.

$$g(x,y) \text{ is classifed as } \begin{cases} \text{"binary 1" if } \mu[g(x,y)] \ge 0.5 \\ \text{"binary 0" otherwise.} \end{cases} \quad (16)$$

Step 6: Repeat from step 1 to step 5 for all salient regions.

Step 7: A pixel can be contained in many different ROIs because some ROIs lay upon another ROI. A pixel can be classified as "binary 1" in some ROIs and same pixel can be classified as "binary 0" in different ROIs by (16). We count classification results due to different ROIs of a pixel and adopt the dominant one as a final decision result. Our criterion to make a final decision is defined as (17).

$$\text{if } \sum \#_1\{g(x,y)\} \ge \sum \#_0\{g(x,y)\}$$
$$g(x,y) \text{ is classifed as } \begin{cases} \text{"potential target pixel"} \\ \text{"background pixel" otherwise,} \end{cases} \quad (17)$$

where $\#_1\{g(x,y)\}$ denotes the number of cases of that $g(x,y)$ is classified as "binary 1" by (16). $\#_0\{g(x,y)\}$ is defined by the similar manner for "binary 0".

Figure 8 shows the result of local thresholding of Fig. 1.

C. Binary template matching

As shown in Fig. 8, the thresholding result has many potential target chips that contain small number of true targets and many clutter chips. Therefore, clutter rejection is necessary to identify true targets by discarding the clutter chips (false alarms) from the potential target chips.

Therefore, we use a prior knowledge and binary template matching technique to remove clutters from the thresholding result. A prior knowledge is maximum and minimum target size. In our implementation, maximum and minimum target sizes are 30 × 15 pixels and 10 × 8 pixels, respectively. To generate target templates, we manually divide some binary images of true target chips into two groups by target size. Binary templates are made by two sequential operations for each group. At first, centroids of binary target images are aligned. Then binary OR operation is applied for each pixel position of binary images. Two binary templates are shown in Fig. 9.

We define a measure of affinity to determine correlation between the templates and potential target chips. Affinity is defined by

$$M_a = \left[\frac{\#(T \text{ AND } B)}{\#(T \text{ XOR } B) + 1} \right], \quad (18)$$

where $\#(X)$ denotes the number of pixels with 1 in the binary image X. T is a binary template image and B is a binary image of potential target chips given as Fig. 8. AND and XOR represent binary AND and exclusive OR operation, respectively. Clutter rejection procedure by binary template matching is such as:

Step 1: Label the binary images of thresholding result. Size, centroid and circumscribed rectangle of the binary objects are computed in the labeling.

Step 2: If the circumscribed rectangle of a binary object is larger than the circumscribed rectangle of template A, the object is excluded from the next steps.

Because width of military vehicles is mostly longer than height, the object with longer height than width is excluded from the next steps.

Step 3: Measure affinity criterion by (18) for a binary object. If the size of a binary object is larger than a half of the template A, template A is used to compute M_a value. Otherwise, template B is used in calculating M_a value. If M_a is greater than T_1, the object is classified as a true target. Otherwise, the component is classified as background. T_1 is 0.5 in our implementation. Parameter T_1 affects detection rate and false alarms.

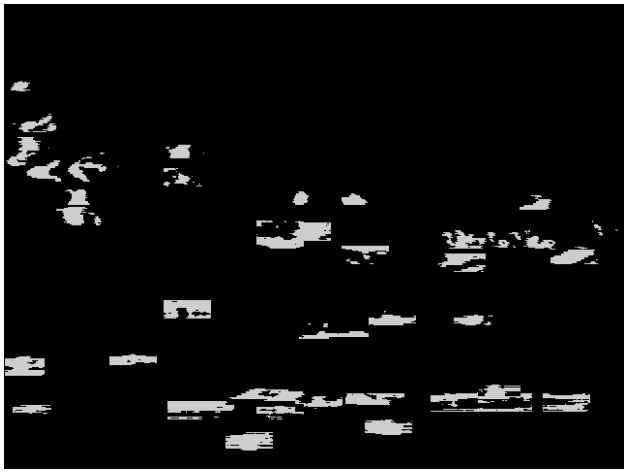

Figure 8. Result of local thresholding of Fig. 1

Template A Template B

Figure 9. Two binary templates

Step 4: Repeat from step 1 to step 3 for all binary objects.

When binary template matching and affinity measure are applied to Fig. 8, most of clutters are rejected as shown in Fig. 10(a). The leftmost binary object in Fig. 10(a) is a clutter but is not rejected because the shape of the object is very similar to templates. Figure 10(b) shows the enlarged region of the white rectangle of Fig. 10(a). The leftmost crosshair is a false alarm and the other crosshairs are center of the detected targets. However, a true target in the rightmost in Fig. 10(b) is false rejected.

III. EXPERIMENTS

The imaging sensor for this experiment was an infrared thermal sight that was installed in an army vehicle. The environment was natural field that was used a training site for battle tanks. Images were gathered in various conditions, i.e., different seasons, different times of the day, engine on/off, various aspect angles. The types of targets were three battle tanks, two armored infantry vehicles, and a truck. In the database, the aspect angle of the targets was from 0° to 360° and the elevation angle of military vehicles was nearly zero. The imaging sensor was located at a distance of about 1.1~1.5 Km from targets. The twenty-four test images were selected from FLIR image data of Agency for Defense Development (ADD) in Korea. Test images are low contrast and high cluttered images. They include seventy-six targets in total. On an average, an image includes about three targets as shown in Fig. 11(a). Figure 11(a) shows an example of medium cluttered image with three targets.

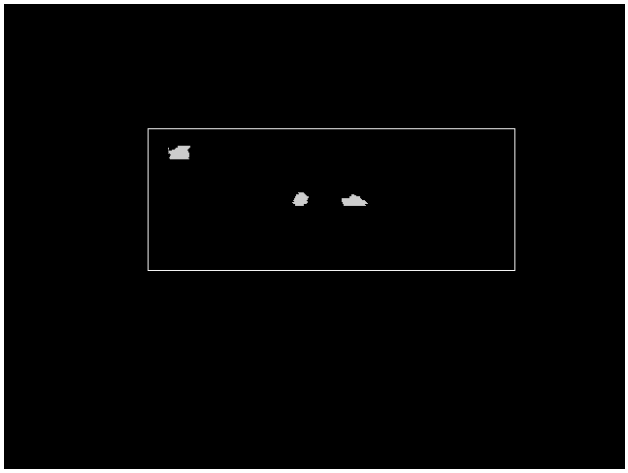

(a)

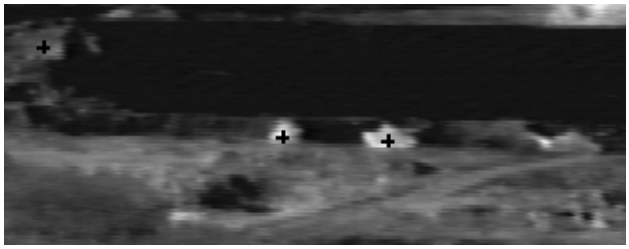

(b)

Figure 10. Result of binary template matching of Fig. 1

The result of local thresholding and clutter rejection is shown in Fig. 11(b). Figure 11(c) shows the final result of target detection. The leftmost crosshair is a false alarm and the other crosshairs are center of the detected targets. Figure 12(a) is a high cluttered image with five targets. The result of thresholding and clutter rejection is shown in Fig. 12(b). Figure 12(c) is the final result that shows four detected targets, a false rejected target and a false alarm. Figure 13(a) is a low contrast image with three targets. The result of target detection is shown in Figs. 13(b) and 13(c). The detection results from Fig. 10 to Fig. 13 are obtained by all same parameters for T_0, ω_{th} and T_1.

We evaluate the performance of the proposed method in terms of a receiver operating characteristic (ROC) curve. For a potential target image two events can be defined, i.e., either the potential target is a real target (event "T") or it is a clutter (event "C"). When a potential target image is presented to a target detection system, the system outputs by answering "yes" (Y) meaning that it is a real target; or "no" (N) meaning that it is a clutter. The detection rate is the probability of responding "yes" given an event "T". Otherwise, the probability of responding "yes" given an event "C" is called the false alarm rate [24]. Thus,

$$\text{Detection rate} = P(Y \mid T), \tag{19}$$

$$\text{False alarm rate} = P(Y \mid C). \tag{20}$$

To evaluate the performance, the proposed method was compared with morphological method [21] which has been used in many ATR systems. For fair comparison of these two methods, clutter rejection method in Sec. II.C was added to the original morphological method in the Ref. [21]. Probability of target detection and the number of false alarms per scene can be varied by tuning

algorithm parameters such as ω_{th} and T_1 in our method. Test results were demonstrated by the ROC curve as shown in Fig. 14. Detection rate of morphology algorithm was 54 % but our target detector achieved 78 % detection rate with 2.0 false alarms per image. Meanwhile, computation time is also important to implement a target detector in real-time ATR system. In 2.0 false alarm rate per image, average computation time was 0.8 second in our method but 1.2 second in morphological method. It was measured by a Pentium III personal computer with 1.5 giga Hz clock and 512 mega bytes memory.

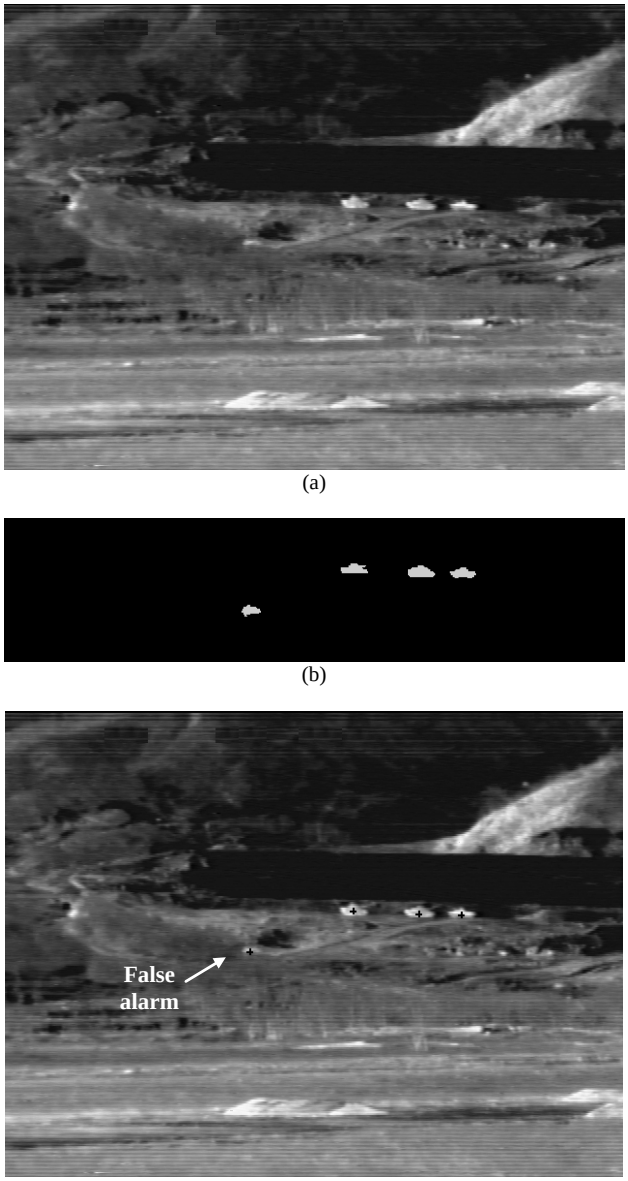

(a)

(b)

(c)

Figure 11. (a) An example of medium cluttered image, (b) the result of thresholding and clutter rejection, (c) final result of target detection

IV. CONCLUSION

This paper proposed a new target detection method which can be applied to the intelligent army vehicles in the ground-to-ground scenario. In the initial target detection stage, potential targets should not be missed to minimize incorrect rejection rate and center of targets should be found in many ATR systems such as automatic target tracker. In that sense, proposed center-surround difference with adaptive threshold and local thresholding is good to extract potential targets and find centers. The proposed method was tested in many natural images which were gathered in natural field with various environmental conditions. The experimental results proved that our proposed method is suitable for detecting small targets in FLIR images.

We will adapt the proposed method to a military system in the near future.

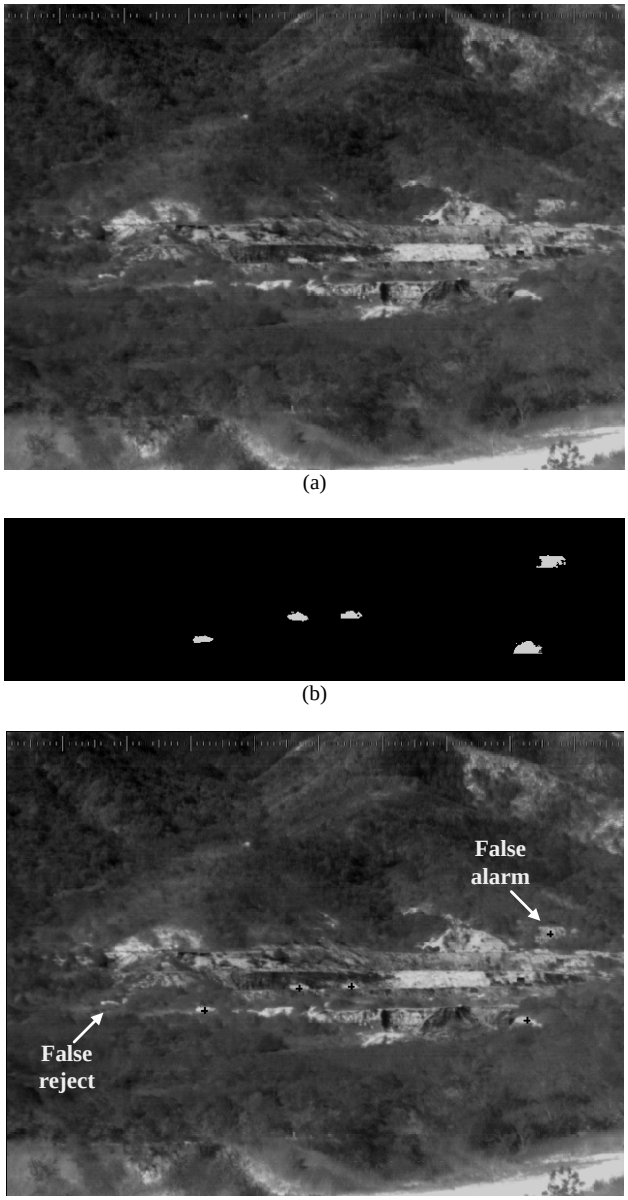

(a)

(b)

(c)

Figure 12. (a) An example of high cluttered image, (b) the result of thresholding and clutter rejection, (c) final result of target detection

(a)

(b)

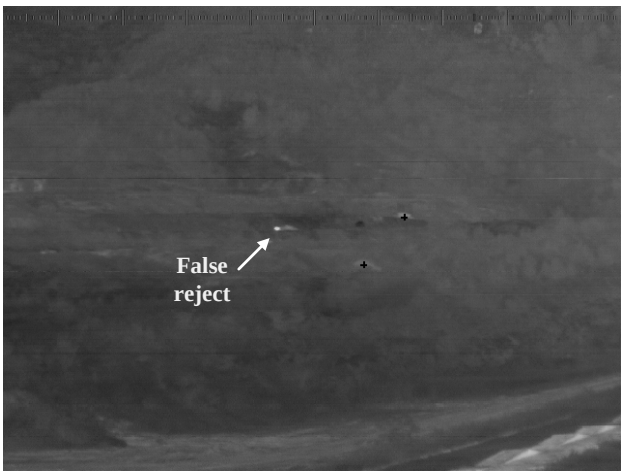

(c)

Figure 13. (a) An example of low contrast image, (b) the result of thresholding and clutter rejection, (c) final result of target detection

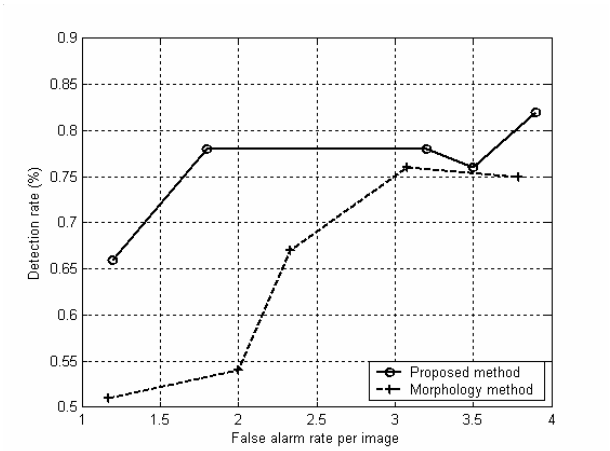

Figure 14. Comparison of ROC performance

REFERENCES

[1] B. Bhanu, "Automatic target recognition: state of the art survey," *IEEE Trans. Aerosp. Electron. Syst.*, vol. 22, no. 4, pp. 364-379, 1986.

[2] M. W. Roth, "Survey of neural network technology for automatic target recognition," *IEEE Trans. Neural Networks*, vol. 1, no. 1, pp. 28-43, 1990.

[3] S. K. Rogers, J. M. Colombi, C. E. Martin, J. C. Gainey, K. H. Fielding, T. J. Burns, D. W. Ruck, M. Kabrisky and M. Oxley, "Neural networks for automatic target recognition," *Neural Networks*, vol. 8, no. 7, pp. 1153-1184, 1995.

[4] J. A. Racher, C. P. Walters, R. G. Buser, and B. D. Guenther, "Aided and automatic target recognition based upon sensory inputs from image forming systems," *IEEE Trans. Patt. Anal. and Mach. Intell.*, vol. 19**,** no. 9, pp. 1004-1019, 1997.

[5] D. Casasent and A. Ye, "Detection filters and algorithm fusion for ATR," *IEEE Trans. Image Process.*, vol. 6, no. 1, pp. 114-125, 1997.

[6] X. Wu and B. Bhanu, "Gabor wavelet representation for 3-D object recognition," *IEEE Trans. Image Process.* vol. 6, no. 1, pp. 47-64, 1997.

[7] B. Ernisse, S. K. Rogers, M. P. Desimio and R. A. Raines, "Complete automatic target cuer/recognition system for tactical forward-looking infrared images," *Opt. Eng.*, vol. 36, no. 9, pp. 2593-2603, 1997.

[8] L. C. Wang, S. Z. Der and N. M. Nasrabadi, "Automatic target recognition using a feature-decomposition and data-decomposition modular neural network," *IEEE Trans. Image Process.*, vol. 7, no. 8, pp. 1113-1121, 1998.

[9] R. G. Driggers, P. Cox and T. Edwards, *Introduction to infrared and electro-optical systems*, Artech house, Boston, 1999.

[10] D. Nair and J. K. Aggarwal, "Bayesian recognition of targets by parts in second generation forward looking infrared images," *Image and Vis. Comput.*, vol. 18, pp. 849-864, 2000.

[11] S. G. Sun and H. W. Park, "Automatic target recognition using target boundary information in FLIR images", *Proc. The IASTED Int. Conf. Signal and Image Processing*, vol. 1, pp. 405-410, 2000.

[12] S. G. Sun and H. W. Park, "Segmentation of forward-looking infrared image using fuzzy thresholding and edge detection", *Opt. Eng.*, vol. 40, no. 11, pp. 2638-2645, 2001.

[13] S. G. Sun and H. W. Park, "Invariant feature extraction based on radial and distance function for automatic target recognition", *Proc. IEEE Int. Conf., Image Processing*, vol. 3, pp. 345-348, 2002.

[14] S. G. Sun and H. W. Park, "Automatic target recognition using boundary partitioning and invariant features in FLIR images," *Opt. Eng.*, vol.42, no.2, pp. 524-533, 2003.

[15] D. S. Jun, S. G. Sun and H. W. Park, "An automatic target detection using binary template matching," *Opt. Eng.*, vol. 44, no. 3, pp. 036401-1~036401-7, 2005.

[16] S. G. Sun, D. M. Kwak, W. B. Jang and D. J. Kim, "Small target detection using center-surround difference with locally adaptive threshold," *Proc. IEEE, Int. Symp., Image and Signal Processing and Analysis*, vol. 1, pp. 402-407, 2005.

[17] D. Casasent and J. Smokelin, "Real, imaginary, and clutter Gabor filter fusion for detection with reduced false alarm," *Opt. Eng.*, vol. 33, no. 7, pp. 2255-2263, 1994.

[18] S. A. Rizvi, T. N. Saadawi, and N.M. Nasrabadi "A modular clutter rejection technique for FLIR imagery using region-based principal component analysis," *IEEE Image Processing*, vol. 2, pp.475-478, 2000.

[19] L. A. Chan, S. Z. Der and N. M. Nasrabadi, "Improved target detector for FLIR imagery," *Proc. IEEE ICASSP*, vol. 2, pp. 401-404, 2003.
[20] L. A. Chan, S. Z. Der and N. M. Nasrabadi, "Automatic target detection using dualband infrared imagery," *Proc. IEEE ICASSP*, vol.6, pp. 2286-2289, 2000.
[21] Q. H. Pham, T. M. Brosnan and M. J. T. Smith, "Sequential digital filters for fast detection of targets in FLIR image data," *Proc. SPIE*, vol. 3069, pp. 62-73, 1997.
[22] R. Murenzi, *et. al.* "Detection of targets in low resolution FLIR imagery using two-dimensional directional wavelets," *Proc. SPIE*, vol. 3371, pp. 510-518, 1998.
[23] S. A. Rizvi, N. M. Nasrabadi, and S. Z. Der, "A clutter rejection technique for FLIR imagery using region-based principal component analysis," *Proc. SPIE*, vol. 3718, pp. 57-66, 1999.
[24] L. A. Chan, N. M. Nasrabadi and D. Torrieri, "Bipolar eigenspace separation transformation for automatic clutter rejection," *Proc. IEEE Int. Conf., Image Processing*, vol. 1, pp. 139-142, 1999.
[25] L. Itti, C. Koch and E. NieBur, "A model of saliency-based visual attention for rapid scene analysis," *IEEE Trans. Patt. Anal.*, vol. 20, no. 11, pp. 1254-1259, 1998.
[26] U. Braga-Neto, M. Choudhary and J. Goutsias, "Automatic target detection and tracking in forward-looking infrared image sequences using morphological connected operators," *J. Elect. Imaging*, vol. 13, no. 4, pp. 802-812, 2004.
[27] J. Burt and E. H. Adelson, "The Laplacian pyramid as a compact image code," *IEEE Trans. Communication*, vol. 31, no. 4, pp. 532-540, 1983.
[28] K. Jain, *Fundamentals of digital image processing*, Prentice Hall, 2003.

Sun-Gu Sun received his BS and MS degrees in electrical engineering in 1987 and 1989 from Hanyang University and PhD degree in electrical engineering in 2003 from Korea Advanced Institute of Science and Technology (KAIST), Korea.

He has worked as a researcher of senior member at Agency for Defense Development (ADD) in Korea since 1989. His professional experience has been concentrated on developing fire control and command control system in military application. Especially, his current research interest includes image processing, robot vision, sensor fusion, target detection, tracking and recognition.

Dong-Min Kwak received his BS and MS degrees in electronic engineering from Kyungpook National University, Taegu, Korea, in 1997 and 1999 and PhD degree at the graduate school of electronics in Kyungpook National University.

He has been a researcher of senior member at Agency for Defense Development (ADD) in Korea since 2004. His research interests include target detection and recognition, image stabilization, content-based image retrieval, medical image processing and computer-aided diagnosis.